

## REVERSE CURRENT-VOLTAGE CHARACTERISTICS OF METAL-SILICIDE SCHOTTKY DIODES

J. M. ANDREWS and M. P. LEPSALTER

Bell Telephone Laboratories, Murray Hill, New Jersey 07974, U.S.A.

(Received 10 November 1969; in revised form 18 December 1969)

**Abstract**—The soft behavior of reverse biased Schottky barrier diodes has often been difficult to interpret quantitatively. The development of metal-silicide devices with diffused guard rings has made it possible to verify experimentally an advanced theoretical model. Reverse characteristics can now be accurately predicted over wide ranges of current, voltage, barrier height and temperature. The theoretical description accounts for anisotropy of effective masses, scattering by optical phonons, and quantum mechanical reflection and tunneling at the metal-semiconductor interface. These considerations yield practical Richardson constants equal to 112 for electrons and 32 for holes in silicon. Absence of true saturation in the reverse characteristic is caused by an electric field dependence of the effective barrier height. In addition to the usual image-force correction, the barrier height is lowered by a newly recognized effect attributed to an electrostatic dipole layer at the metal-semiconductor interface. Experimental devices have been fabricated using RhSi, ZrSi<sub>2</sub>, and PtSi contacts, forming barriers in both *n*- and *p*-type silicon. The resulting structures have been found to be extremely stable and uniform; furthermore, the metal-semiconductor interface, produced by solid-solid chemical reaction, is believed to be free from intervening layers of oxide and other contaminants. When necessary to eliminate field-enhancement at the electrode periphery, diffused guard rings have been incorporated into the structures. Agreement between experimental data and theory is obtained over nearly five orders of magnitude in reverse bias and eleven orders of magnitude in reverse current density, usually with an rms deviation of less than 10 per cent.

**Résumé**—Le comportement doux de diodes de barrière Schottky à polarisation inverse a souvent été difficile à interpréter quantitativement. Le développement de dispositifs de silicides métalliques avec des cercles protecteurs diffusés a permis la vérification expérimentale d'un modèle théorique avancé. Les caractéristiques d'inversion sont maintenant précisément prévisibles sur des gammes étendues de courant, de tension, de hauteur de barrière, et de température. La description théorique explique l'anisotropie des masses effectives, la dispersion par phonons optiques et le percement et la réflexion mécanique quantique à l'interface métal-demi conducteur. Ces considérations donnent des constantes de Richardson pratiques égales à 112 pour les électrons et à 32 pour les trous dans le silicium. L'absence de véritable saturation dans la caractéristique à inversion est due à la dépendance d'un champ électrique sur la hauteur effective de la barrière. En plus de la correction habituelle image-force, la hauteur de barrière est réduite par un effet nouvellement reconnu attribué à une couche dipolaire électrostatique à l'interface métal-semi conducteur. Des dispositifs expérimentaux ont été fabriqués avec des contacts en RhSi, en ZrSi<sub>2</sub> et en PtSi, formant des barrières dans les siliciums du type *n* aussi bien que du type *p*. Les structures qui en résultent sont trouvées être extrêmement stables et uniformes; de plus, l'interface métal-semi conducteur produite par une réaction chimique solide-solide est pensée être dépourvue de couches d'intervention d'oxyde et autres contaminants. Lorsqu'il est nécessaire d'éliminer des concentrations de champ sur la périphérie des électrodes, des cercles protecteurs diffusés sont incorporés dans les structures. On obtient un accord entre les données expérimentales et la théorie sur près de cinq ordres de grandeur en polarisation inverse et onze ordres de grandeur en densité de courant inverse, normalement avec une déviation de la racine moyenne carrée de moins de 10 pour cent.

**Zusammenfassung**—Der weiche Durchbruch von Schottky-Dioden ist meist schwierig quantitativ zu beschreiben. Die Entwicklung von Metallsilizid-Strukturen mit eindiffundiertem Schutzring hat es nun ermöglicht ein verbessertes Modell experimentell zu prüfen. Die Sperrcharakteristiken

können jetzt sehr genau vorhergesagt werden in einem weiten Bereich für Strom, Spannung, Barrierenhöhe und die Temperatur. Die theoretische Beschreibung berücksichtigt die Anisotropie der effektiven Massen, die Streuung an optischen Phononen sowie die quantenmechanische Reflexion und den Tunneleffekt an der Grenzfläche zwischen Metall und Halbleiter. Die Betrachtungen liefern praktische Werte für die Richardson Konstante von 112 für Elektronen und 32 für Löcher in Silizium. Die fehlende Sättigung in der Sperrkennlinie wird durch die Feldabhängigkeit der effektiven Barrierenhöhe hervorgerufen. Zur gewohnten Bildkraftkorrektur kommt noch eine Barrierenabsenkung durch den neuerlich erkannten Einfluss einer elektrostatischen Dipolschicht an der Metall-Halbleiter-Grenzfläche. Proben wurden hergestellt mit RhSi-, ZrSi<sub>2</sub>- und PtSi-Kontakten, die sowohl mit *n*- als auch mit *p*-Typ-Silizium eine Barriere bilden. Die gewonnenen Strukturen waren extrem stabil und gleichmässig und es wird vermutet, dass die durch chemische Festkörperreaktion gebildete Metall-Halbleiter-Grenzfläche frei ist von Zwischenschichten aus Oxiden und anderen Verunreinigungen. Wenn es nötig war, wurde die Felderhöhung an der Randzone der Elektroden durch einen in die Struktur eindiffundierten Schutzring beseitigt. Übereinstimmung zwischen Theorie und Experiment ergab sich über einen Bereich von nahezu fünf Grössenordnungen für die Sperrspannung und von elf Grössenordnungen für die Sperrstromdichte bei einer Abweichung von meist weniger als 10 Prozent.

### NOTATION

- $A_o$  = ideal Richardson constant for metal-vacuum interface ( $A\text{ cm}^{-2}\text{ }^\circ\text{K}^{-2}$ ).  
 $A^*$  = effective Richardson constant for emission into medium with anisotropic effective mass of carriers ( $A\text{ cm}^{-2}\text{ }^\circ\text{K}^{-2}$ ).  
 $A^{**}$  = effective Richardson constant for metal-semiconductor interface ( $A\text{ cm}^{-2}\text{ }^\circ\text{K}^{-2}$ ).  
 $d$  = thickness of intervening layer of oxide or contamination at nonideal metal-semiconductor interface (cm).  
 $\mathcal{E}_m$  = maximum electrostatic field at metal-semiconductor interface ( $V\text{ cm}^{-1}$ ).  
 $f_P$  = probability of electron (or hole) transmission through a potential barrier in the presence of scattering by optical phonons.  
 $f_Q$  = probability of electron (or hole) transmission through a potential barrier in the presence of quantum mechanical reflection or tunneling.  
 $h$  = Planck's constant (J sec).  
 $J_R$  = reverse current density ( $A\text{ cm}^{-2}$ ).  
 $J_S$  = saturation current density ( $A\text{ cm}^{-2}$ ) (academic case, no barrier-lowering mechanism).  
 $J'_S$  = quasi-saturation current density ( $A\text{ cm}^{-2}$ ) (practical case, with barrier lowering).  
 $k$  = Boltzmann's constant ( $J\text{ }^\circ\text{K}^{-1}$ ).  
 $l_i^2$  = direction cosine with respect to *i*th principal axis.  
 $m$  = rest mass of electron in free space (g).  
 $m_j^*$  = *j*th component of effective mass tensor with respect to principal axis of semiconductor (gm).  
 $n_s$  = density of surface states at silicon-silicon dioxide interface ( $\text{eV}^{-1}\text{ cm}^{-2}$ ).  
 $q$  = electronic charge (C).  
 $T$  = absolute temperature ( $^\circ\text{K}$ ).  
 $v_D$  = effective diffusion velocity in depletion layer at metal-semiconductor interface ( $\text{cm sec}^{-1}$ ).  
 $v_R$  = effective recombination velocity between potential barrier maximum and metal-semiconductor interface ( $\text{cm sec}^{-1}$ ).

- $V_R$  = reverse bias (V).  
 $\alpha$  = rate of change of electrostatic barrier height with respect to electric field (cm).  
 $\gamma$  = fraction of metal-semiconductor potential barrier attributable to difference between work function  $\varphi_m$  and electron affinity  $\chi_s$ .  
 $\epsilon_i$  = electrical permittivity of intervening layer of oxide or contamination at nonideal metal-semiconductor interface ( $F\text{ cm}^{-1}$ ).  
 $\epsilon_s$  = electrical permittivity of semiconductor ( $F\text{ cm}^{-1}$ ).  
 $\varphi_B$  = effective potential barrier at metal-semiconductor interface (eV).  
 $\varphi_{BO}$  = effective potential barrier at metal-semiconductor interface for vanishing electric field, or flatband case (eV).  
 $\varphi_g$  = forbidden energy gap of semiconductor (eV).  
 $\varphi_m$  = work function of metal (eV).  
 $\varphi_o$  = equilibrium level of occupied surface states of semiconductor (eV).  
 $\chi_s$  = electron affinity of semiconductor (eV).

### 1. INTRODUCTION

THE ABSENCE of true saturation in the reverse current of metal-semiconductor (Schottky) barriers has been difficult to interpret on theoretical grounds. Soft reverse characteristics are observed in metal-silicide barriers even when diffused guard rings are used to eliminate premature breakdown induced by the enhanced electric field at the periphery of the devices. Reverse characteristics of metal-silicide Schottky diodes are here shown to be consistent with an improved model. Agreement between theory and experiment is demonstrated for reverse voltages ranging from 1 mV to the onset of avalanche or tunneling breakdown.

The basic current transport mechanism is thermionic emission over the potential barrier at

the metal-semiconductor interface, modified by anisotropy of the effective masses of the carriers, scattering by optical phonons, and quantum mechanical reflection and tunneling. These considerations yield different values for the effective Richardson constant for electrons and holes, which are slightly dependent upon the electric field at the metal-semiconductor interface. However, this field-dependence, together with image-force lowering of the effective barrier height, is insufficient to fully account for the soft nature of the reverse characteristics. A further correction, attributed to a dipole layer at the metal-semiconductor interface, is required in order to bring theory into agreement with experiment.<sup>(1)</sup> Other workers have previously postulated a dipole layer for the Al:nGaAs interface caused by an exponential charge distribution associated with surface states.<sup>(2)</sup> In other cases the dipole moment can be attributed to a layer of oxide or contamination between the metal and the semiconductor.<sup>(3)</sup> However, the fabrication process for forming metal-silicide contacts in silicon virtually eliminates problems of contamination and surface imperfections.<sup>(4,5)</sup> Soft behavior of metal-silicide barriers is attributed to penetration of electronic wave functions from the metal into the forbidden gap of the semiconductor. The dipolar barrier lowering effect can often be approximated by a single term, linear in electric field.

The combination of new values for the effective Richardson constant and the image-force and dipolar corrections for the effective barrier height leads to quantitative agreement between theory and experiment with rms deviation usually less than 10 per cent. Experiments have been carried out on PtSi, RhSi, and ZrSi<sub>2</sub> contacts formed in both *n*- and *p*-type silicon. These diodes are formed by solid-solid chemical reaction between the metal and silicon, causing the metallurgical interface to move into the interior of the silicon lattice away from surface imperfections and contamination. The thermodynamic stability and chemical nature of these bonded contacts have been discussed in detail elsewhere.<sup>(4)</sup> The reproducibility and uniformity of the resulting improved junctions, particularly when guard rings are used, made such detailed observations feasible.

Section 2 contains a theoretical discussion of the concepts of an effective Richardson constant and

an effective barrier height, both germane to the physical process of thermionic emission over the potential barrier existing at an ideal metal-semiconductor interface. Experimental results for a number of representative metal-silicide devices (PtSi, RhSi, and ZrSi<sub>2</sub>) formed in *n*- and *p*-type silicon are presented in Section 3. Comparison between theory and experiment for fixed temperatures ranging from 276 to 344°K is shown, spanning five orders of magnitude in reverse bias voltage and eleven orders of magnitude in reverse current density. A summary and suggestions for further research are included in Section 4.

## 2. THEORY

The principle underlying current transport in metal-semiconductor barriers is closely analogous to the thermionic emission of electrons into a vacuum. The formulation of this problem leads to the equation of RICHARDSON and DUSHMAN.<sup>(6)</sup>

$$J_R = A^{**} T^2 \exp(-q\varphi_B/kT)[1 - \exp(-qV_R/kT)]. \quad (1)$$

Three features distinguish this result from the metal-vacuum case:

1. The effective Richardson constant  $A^{**}$  can deviate greatly from the free-space value of  $120 \text{ A cm}^{-2} \text{ }^\circ\text{K}^{-2}$ .
2. The value of  $A^{**}$  for a metal-semiconductor interface is not really constant, but varies somewhat, depending upon the maximum value of the electric field in the depletion region of the semiconductor.
3. The effective barrier height  $\varphi_B$  can vary somewhat more rapidly with electric field than the usual image-force model would predict.

The discussion in 2.1 will show that the dominant consideration pursuant to  $A^{**}$  lies in the contrasting magnitudes for *n*- and *p*-type silicon. The electric field dependence of  $A^{**}$  is small over the actual range of values encountered in the metal-silicide devices studied. Small variations in  $\varphi_B$ , however, are much more important because of its exponential behavior. The origin of the parametric dependence of  $\varphi_B$  on electric field is presented in 2.2.

### 2.1. Effective Richardson constant

For the simple case of an electron, thermally emitted from a metal into a vacuum, the proportionality factor in equation (1) is composed of fundamental constants.

$$A_0 = 4\pi m q k^2 / h^3. \quad (2)$$

The effective Richardson constant in Schottky barrier rectification differs from the metal-vacuum value ( $120 \text{ A cm}^{-2} \text{ }^\circ\text{K}^{-2}$ ) for three important reasons:

1. The dynamics of electrons or holes, thermally emitted over a potential barrier from a metal into a semiconductor, are characterized by an effective mass  $m^*$  or, more specifically, an appropriate combination of the components of the effective mass tensor for the semiconductor.
2. Electrons or holes emitted into the high-field region near the metal-semiconductor interface are scattered by optical phonons.
3. The electric permittivities of most semiconductors are typically an order of magnitude greater than that of vacuum. This sharpens the potential barrier profile accordingly, and the quantum mechanical transmission through, or the reflection by, such an accentuated potential profile is greatly enhanced.

The special kinetic processes governing carrier transport at a metal-semiconductor interface are illustrated schematically in Fig. 1.

In an anisotropic semiconductor, the details of the result of carrier effective mass on thermionic emission across the metal-semiconductor interface have been calculated by CROWELL.<sup>(7)</sup> The relationship given by equation (2) is written in tensor form.

$$A^* = \frac{4\pi q k^2}{h^3} (l_i^2 m_j^* m_k^*)^{1/2}. \quad (3)$$

This is summed, first over permuted indices, then over equivalent minima in wave-vector space. The quantity  $l_i$  is the direction cosine of the current density relative to one of the principal axes of the effective mass tensor, represented by  $m_j^*$ . A summary of the mass tensor dependence of the effective Richardson constant in *n*- and *p*-type silicon of two orientations is contained in Table 1.

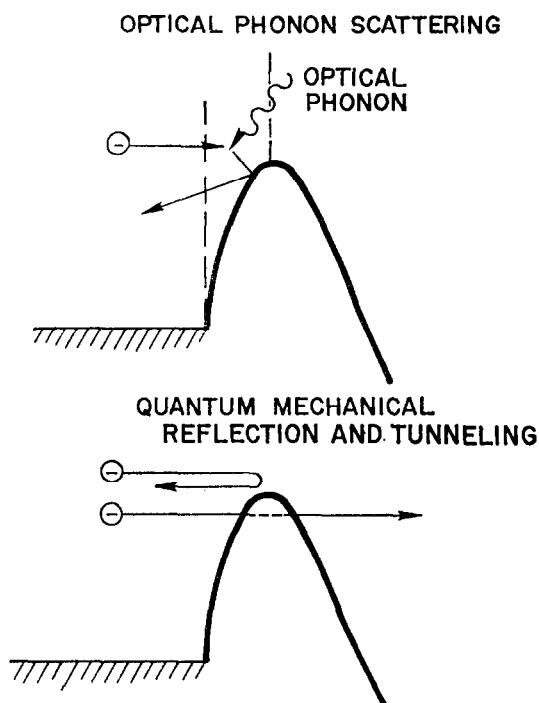


FIG. 1. Schematic representation of the kinetic processes, existing at a metal-semiconductor interface, which modify the Richardson constant.

These are presented as numerical ratios, relative to the free-space value of the Richardson constant  $A_0$ .

Table 1. Thermionic emission effective masses in silicon

Direction of current	Silicon type	Number of equivalent minima	$A^*/A_0$
$\langle 111 \rangle$	<i>n</i>	6	2.15
$\langle 100 \rangle$	<i>n</i>	$\begin{pmatrix} 4 \\ 2 \end{pmatrix}$	2.05
—	<i>p</i>	—	0.66

The effective Richardson constant at an ideal metal-semiconductor interface is affected by the probability of electron or hole transmission over the potential barrier in the presence of scattering

by optical phonons. This probability, represented by  $f_P$ , has been calculated as a function of electric field for electrons in silicon by CROWELL and SZE.<sup>(6)</sup> The calculation has been repeated for holes by one of the present authors.<sup>(9)</sup> Quantum-mechanical transmission and reflection at the interface have also been treated by CROWELL and SZE,<sup>(10)</sup> who presented their result  $f_Q$  as a function of electric field.<sup>(8)</sup> In their thermionic-diffusion theory, Crowell and Sze define an effective Richardson factor  $A^{**}$  that is useful for practical device design considerations.

$$A^{**} = \frac{f_P f_Q}{1 + f_P f_Q v_R / v_D} A^*. \quad (4)$$

The electric field dependence of  $A^{**}$  is shown in Fig. 2 for both electrons and holes in moderately doped ( $10^{16}$ ) silicon at room temperature.

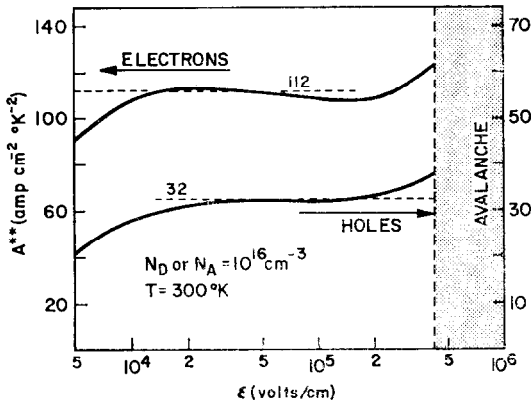


FIG. 2. Electric field dependence of effective Richardson constants of electrons and holes in silicon.

Clearly the values of  $A^{**}$  are nearly constant over the entire range of reverse bias  $V_R$  that can be applied without inducing avalanche breakdown. Accordingly it is expedient to set

$$A^{**} \simeq 112 \text{ (A cm}^{-2} \text{ °K}^{-2} \text{) electrons}$$

$$A^{**} \simeq 32 \text{ (A cm}^{-2} \text{ °K}^{-2} \text{) holes.}$$

These values have provided a good quantitative basis for contrasting Schottky barrier behavior between  $n$ - and  $p$ -type silicon.<sup>(1,11)</sup>

## 2.2. Effective barrier height

If the potential barrier at a metal-semiconductor

interface were a fixed constant, independent of electric field, the equation for the reverse current density [equation (1)] would exhibit saturation at the value  $J_s$  whenever the reverse bias becomes large in comparison with  $kT/q$ .

$$J_s = A^{**} T^2 \exp(-q\phi_B/kT). \quad (5)$$

Schottky diodes never behave in this way, however, and the reason is based upon the fundamental physical properties of the metal-semiconductor interface. The nature of the interface can be conveniently divided into two distinct aspects: [1] the equilibrium electrostatic charge distribution prevailing at the boundary between metal and semiconductor, presumed to be in intimate contact, and [2] the dynamic charge correlation acting upon carriers thermally emitted over the potential barrier. It has been customary to neglect the detailed electrostatic solution of the metal-semiconductor interface. The problem is difficult and perhaps has been assumed to be of no material consequence. For metal-semiconductor interfaces that are not in intimate contact this may be a valid assumption. In the case of the metallic silicide contact formed in silicon, however, we have good reason to believe that intervening layers of oxide and contaminants are absent. An approximate quantum-mechanical solution<sup>(12)</sup> to the equilibrium charge distribution of an ideal metal-semiconductor interface indicates that the potential barrier is slightly dependent upon electric field. This is in agreement with our experimental results on three metallic silicides grown in both  $n$ - and  $p$ -type silicon to be presented in Section 3. Derivation of this contribution to the electric field dependence of barrier height  $\phi_B$  is outside the scope of this paper. We can anticipate the result, however. Changes in barrier height are small and therefore can be expanded in a Maclaurin series

$$(\Delta\phi_B)_{\text{static}} \doteq \alpha \mathcal{E}_m + \dots \quad (6)$$

The quantity  $\alpha \equiv \partial\phi_B/\partial\mathcal{E}_m$  will be treated as an adjustable empirical parameter in Section 3.

The concept of an image potential acting upon a charge carrier in the vicinity of a metallic surface has been an accepted classical approach to account for the rather complicated electron-electron correlation effects that must exist at an ideal metal-semiconductor interface. Our experimental data

are consistent with retention of this approximate correction to the effective barrier height, utilizing the dynamic dielectric constant which, for silicon, is close to the static value.<sup>(13)</sup>

$$(\Delta\varphi_B)_{\text{image}} = (q\phi_m/4\pi\epsilon_s)^{1/2}. \quad (7)$$

However, the inadequacy of the image potential alone to account for the electric field dependence of the barrier height  $\varphi_B$  is illustrated for two metal-silicide barriers in Fig. 3.

At this point it is necessary to point out an important special case that can occur with practical Schottky diodes formed between silicon and

metals that do not react chemically. Sometimes soft behavior of the reverse characteristics can be explained solely in terms of an image-force correction to the barrier height. This good agreement has been examined by one of the present authors<sup>(9)</sup> in the context of a theory for Schottky barriers formalized by COWLEY and SZE.<sup>(3)</sup> Postulating the existence of a thin, semi-insulating layer of oxide or other contaminant, intervening between a non-reacting metallic contact (gold, aluminum) to silicon, these authors have obtained a relationship between empirical barrier heights and metallic work functions. Implicit in their theory is an

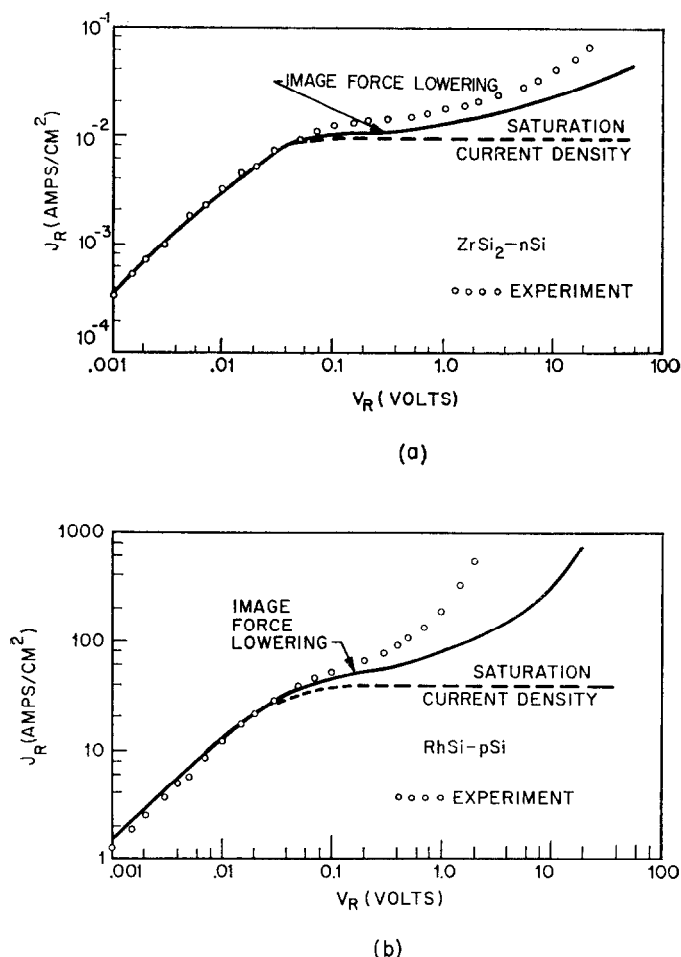


FIG. 3. Failure of image-force concept to fully account for soft reverse characteristics of metal-silicide Schottky diodes. (a)  $\text{ZrSi}_2\text{-nSi}$ ; (b)  $\text{RhSi-pSi}$ .

electric field dependence of the barrier height. It was not, however, retained in their final result because the correction, at zero bias, is very small. In the following equation we have retained the electric field term, because it contributes substantially to effective barrier lowering at moderate and high reverse bias.

$$\varphi_B = \gamma(\varphi_m - \chi_s) + (1 - \gamma)(\varphi_g - \varphi_o) - \alpha \mathcal{E}_m \quad (8)$$

The first term on the right relates the barrier height to the difference between the work function of the metal  $\varphi_m$  and the electron affinity of the semiconductor  $\chi_s$ . The proportionality constant  $\gamma$ , of the order of 0.25, can be determined from a plot of empirical data.<sup>(3,4)</sup> Semiconductor surfaces containing a high density of surface states are likely to have a Fermi level 'pinned' to some value  $\varphi_0$  above the valence band. The second term in the right member of equation (8) incorporates the result of surface states into the effective barrier height. The properties of the interfacial oxide or impurity layer are implicit in the terms  $\gamma$  and  $\alpha$ .

$$\gamma = (1 + 2qdn_s/\epsilon_i)^{-1} \quad (9)$$

$$\alpha = \gamma d \epsilon_s / \epsilon_i \quad (10)$$

Assuming two-fold spin degeneracy, the quantity  $n_s$  represents the density of states at the surface of the silicon;  $d$  and  $\epsilon_i$  are the thickness and electrical permittivity, respectively, of the interfacial oxide or impurity layer. The thickness  $d$  is supposed to be thin enough to allow carrier tunneling, but the static electric field sustained across such a layer can contribute an electric field dependence to the effective barrier height. The magnitude of the proportionality constant  $\alpha$  depends upon the density of surface states  $n_s$ . For large  $n_s$ , the barrier height is pinned to the value  $\varphi_g - \varphi_o$ , and  $\alpha$  vanishes. Thus, in the limit of high surface state density, the reverse characteristics of a nonideal metal-semiconductor interface containing a few monolayers of oxide would be given by an image-force correction alone. The origin of the barrier-lowering term  $\alpha \mathcal{E}_m$  in the case of a nonideal interface [equations (8)–(10)] is distinctly different from the metal-silicide case [equation (6)], but may lead to similar experimental results in the reverse current behavior.

Returning to the more ideal metal-silicide interface, chemically bonded to silicon, let us

summarize the theoretical modifications to the Richardson equation that are needed to bring our theoretical predictions into agreement with experiment. The effective Richardson constant  $A^{**}$  depends upon details of carrier transport in the barrier region; it is slightly field dependent but can be assumed constant within  $\pm 6$  per cent for devices encountered in these investigations. An additional barrier-lowering mechanism, dipolar in origin, is required to explain the soft reverse behavior. The dipole layer is thought to be a fundamental consequence of electronic wave function penetration from the metal into the forbidden gap of the semiconductor.<sup>(12)</sup> Often it is a good approximation to regard the dipolar correction to the barrier height as a linear function of electric field. Typically the dipolar correction is of the same magnitude as the image-force correction (see Fig. 3).

### 3. EXPERIMENT

Successful acquisition of experimental data that yield to the theoretical approach of the preceding section can be attributed both to improvements in fabrication techniques and to the chemical and thermodynamic stability of some of the metallic silicides formed by solid-solid reaction in bulk silicon. Technical details relating to the structure, composition, preparation and metallurgy of metallic silicide barrier devices have been published elsewhere.<sup>(4,5)</sup> In this section experimental data will be presented on three metallic silicide compounds: ZrSi<sub>2</sub>, RhSi and PtSi. Each compound can be formed in both *n*- and *p*-type silicon at a reaction temperature approximately 600–700°C,

Table 2. Metallic silicide Schottky barriers

Metal	Silicon type	Barrier height (eV)	Quasi-saturation current density (A/cm <sup>2</sup> ) (T = 300°K)
ZrSi <sub>2</sub>	<i>n</i>	0.55	$6 \times 10^{-3}$
	<i>p</i>	0.53–0.55	$2-4 \times 10^{-3}$
RhSi	<i>n</i>	0.68–0.70	$2-4 \times 10^{-5}$
	<i>p</i>	0.33	8
PtSi	<i>n</i>	0.85–0.87	$3-6 \times 10^{-8}$
	<i>p</i>	0.25	$2 \times 10^2$

well below the melting points of the corresponding eutectics. In each case the metal is deposited by sputtering onto a silicon surface that had been freshly cleaned by back-sputtering. The compound is then formed by subsequently sintering for five minutes. The six Schottky barriers that can be produced from the three above-mentioned compounds in contact with *n*- and *p*-type silicon span 0.6 eV. The actual values for each are listed in Table 2.

In the context of a soft reverse characteristic, it is perhaps not appropriate to speak of a true saturation current. Nevertheless the concept persists; therefore, a quasi-saturation current is

barrier height  $\phi_B$  evaluated for both *n*- and *p*-type silicon at 300°K.

The physical structure of the experimental devices differ, depending upon the magnitude of the barrier heights. In the case of a low-barrier diode (RhSi-*p*Si, for example), the reverse current density is high, and the series resistance of the silicon can lead to a substantial deviation between the applied bias voltage and the change in the potential appearing across the metal-semiconductor interface. This deviation is minimized by using an epitaxial layer one or two microns thick, grown over degenerate silicon. Such a device is shown in Fig. 5a. High barrier devices, on the

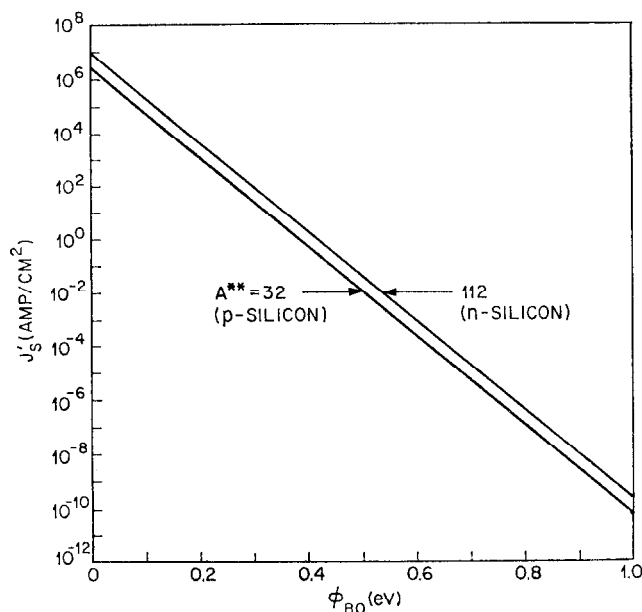


FIG. 4. Quasi-saturation current as a function of barrier height for *n*- and *p*-type silicon.

defined which is not unlike the definition of true saturation [equation (5)].

$$J'_s \equiv \left. \frac{kT}{q} \frac{dJ}{dV} \right|_{V=0} = A^{**} T^2 \exp(-q\phi_B/kT). \quad (11)$$

Values of the quasi-saturation current density for the investigated metal-silicide barriers are also listed in Table 2. Figure 4 shows a plot of quasi-saturation current density  $J'_s$  as a function of

other hand, maintain a strong electric field between the metal contact and the silicon. To prevent premature electrical breakdown at the periphery of the contact, a guard ring is diffused into the silicon substrate prior to formation of the metallic silicide layer. This structure, shown in Fig. 5b, is representative of all diodes formed in *n*-type silicon that were investigated in these experiments. In some cases arrays of diodes were made with diameters ranging from 0.3 to 20 mils



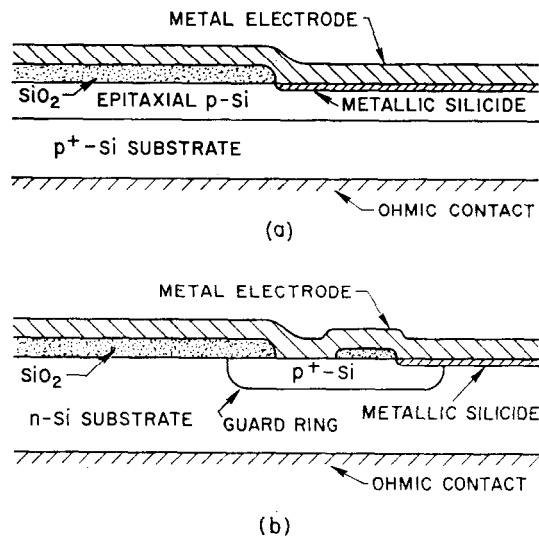


FIG. 5. Structure of metal-silicide Schottky barrier diodes. (a) epitaxial, to reduce series resistance; (b) guard ring, to reduce premature breakdown.

Observations of reverse current were found to scale correctly with the areas of the contact.

### 3.1. Zirconium disilicide

Reverse characteristics of a  $\text{ZrSi}_2$  Schottky diode formed in  $n$ -type silicon are shown in Fig. 6

for three fixed temperatures: 279, 300 and 343°K. Experimental data is shown by the open circles; the solid line represents the theoretical prediction of equation (1) with the barrier height  $\phi_B$  given by the following equation

$$\phi_B = \phi_{BO} - (q\phi_m/4\pi\epsilon_s)^{1/2} - \alpha\phi_m. \quad (12)$$

Parameters of the device shown in Fig. 6 are:  $N_D = 3.5 \times 10^{15} \text{ cm}^{-3}$ ,  $q\phi_{BO} = 0.55 \text{ eV}$ ,  $A^{**} = 112 \text{ A cm}^{-2} \text{ }^\circ\text{K}^{-2}$ ,  $D = 6.9 \times 10^{-3} \text{ cm}$ ,  $\alpha = 15 \text{ \AA}$ . The structure incorporated a  $p$ -type diffused guard ring as illustrated in Fig. 5b. The deviation between the experimental points and the theoretical curves for  $V_R > 30 \text{ V}$  is caused by avalanche multiplication that has not been included in the theory. It should be noted that the ordinate values for  $I_R$  in all plots represent the actual currents observed; no arbitrary scale factors were required. Zirconium disilicide ( $\text{ZrSi}_2$ ) formed in  $p$ -type silicon has a barrier height approximately equal to that for  $n$ -type silicon. Reverse characteristics are quantitatively similar to those for  $\text{ZrSi}_2$ - $n\text{Si}$ , and the data is omitted here.

### 3.2. Rhodium silicide

Experimental and theoretical data for a  $\text{RhSi}$  Schottky diode formed in  $n$ -type silicon are shown in Fig. 7 for three fixed temperatures: 277, 298,

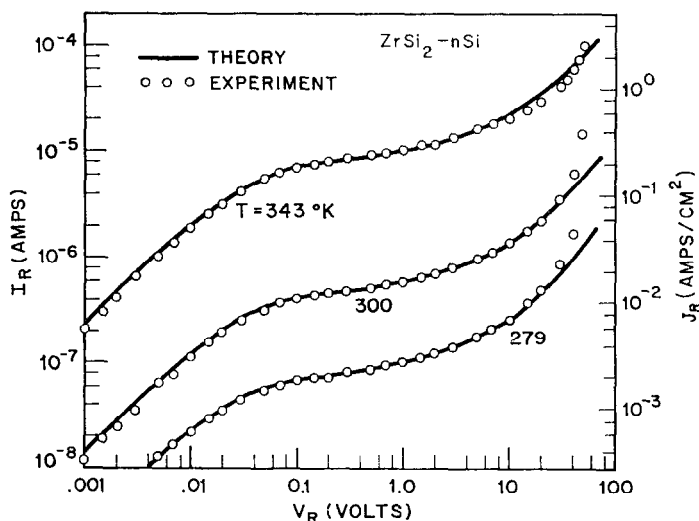


FIG. 6. Reverse characteristics of  $\text{ZrSi}_2$  Schottky diode formed in  $n$ -type silicon.

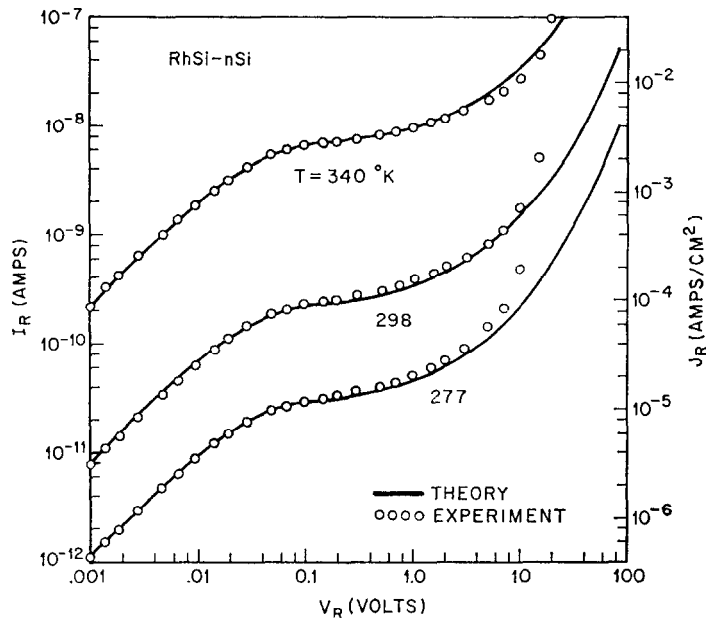


FIG. 7. Reverse characteristics of RhSi Schottky diode formed in *n*-type silicon.

and 340°K. Parameters of the device are:  $N_D = 3.5 \times 10^{15} \text{ cm}^{-3}$ ,  $q\phi_{BO} = 0.68 \text{ eV}$ ,  $A^{**} = 112 \text{ A cm}^{-2} \text{ }^\circ\text{K}^{-2}$ ,  $D = 1.8 \times 10^{-3} \text{ cm}$ ,  $\alpha = 35 \text{ \AA}$ . This device contained a *p*-type diffused guard ring (see Fig. 5b). Good agreement between theory and experiment was obtained up to the region of avalanche multiplication ( $V_R \geq 10 \text{ V}$ ).

Rhodium silicide devices formed in *p*-type silicon do not require a diffused guard ring, but the high current densities encountered at moderate reverse bias cause the series resistance of the silicon to sustain a voltage drop that is a significant fraction of the total bias applied. This problem can be alleviated by utilizing an epitaxial structure such as that shown in Fig. 5a. The theoretical curves shown in Fig. 8 have included the effect of the resistivity of the epitaxial layer ( $\rho = 0.3 \text{ } \Omega\text{-cm}$ ). Observations were made at three temperatures: 276, 297 and 344°K. Parameters of this device are:  $N_A = 9 \times 10^{16} \text{ cm}^{-3}$ ,  $q\phi_{BO} = 0.328 \pm 0.005 \text{ eV}$ ,  $A^{**} = 32 \text{ A cm}^{-2} \text{ }^\circ\text{K}^{-2}$ ,  $D = 1.5 \times 10^{-3} \text{ cm}$ ,  $\alpha = 20 \text{ \AA}$ . At the lowest temperature, deviation between theory and experiment for  $V_R > 2 \text{ V}$  is caused by the transition into the tunneling regime. This behavior is implicit in

the electric field dependence of the effective Richardson constant  $A^{**}$  (see Fig. 2), but is not included in the plot of the theoretical model as illustrated in Fig. 8.

### 3.3. Platinum silicide

Excess reverse current, often an order of magnitude greater than that expected from thermionic emission, is sometimes observed in PtSi barrier diodes formed in *n*-type silicon. The circles in Fig. 9 represent an example of inordinate leakage measured in a PtSi-*n*Si diode at room temperature with a contact diameter equal to  $1.8 \times 10^{-3} \text{ cm}$ . Other device parameters used for calculation of the solid curves:  $N_D = 5.5 \times 10^{15} \text{ cm}^{-3}$ ,  $q\phi_{BO} = 0.85 \text{ eV}$ ,  $A^{**} = 112 \text{ A cm}^{-2} \text{ }^\circ\text{K}^{-2}$ . The reason for the discrepancy between theory and experiment is apparent from the generation mechanism set forth by SAH, NOYCE, and SHOCKLEY to explain the soft reverse characteristics observed in *p-n* junctions.<sup>(14)</sup> According to this model, excess carriers are generated at trap centers, uniformly distributed throughout the depletion region in a reverse-biased junction, and swept out by the high electric field. In the case of very high Schottky

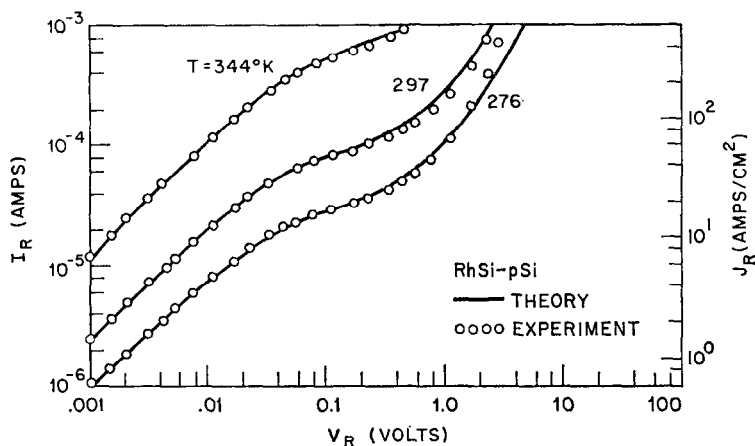


FIG. 8. Reverse characteristics of RhSi Schottky diode formed in *p*-type silicon.

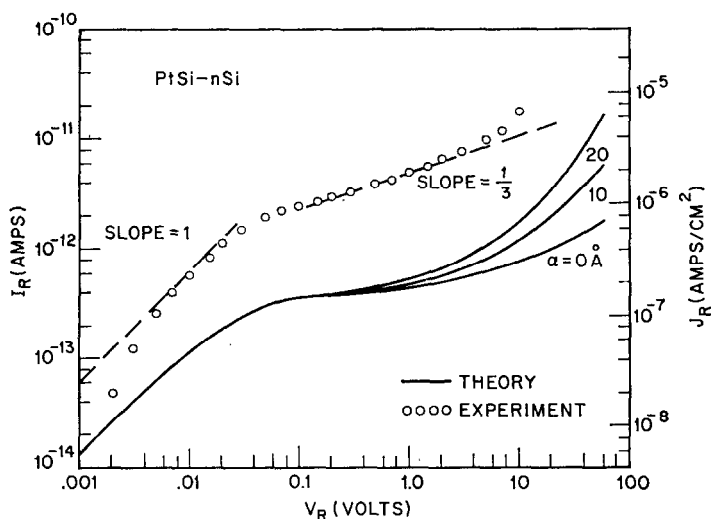


FIG. 9. Reverse characteristics of PtSi Schottky diode formed in *n*-type silicon with short minority carrier lifetime ( $\sim 50$  nsec). Measurements were carried out at room temperature.

barriers (i.e. PtSi-*n*Si : 0.85 eV) formed in silicon that is characterized by short minority carrier lifetime, generation current can exceed the current resulting from thermionic emission over the Schottky barrier. The data shown in Fig. 9 lead to a minority carrier lifetime estimate of the order of 50 nsec.

Experimental observations were repeated for another diode formed in *n*-type silicon with a much longer minority carrier lifetime (32  $\mu$ sec). Agreement between theory and experiment is satisfactory as shown in Fig. 10. Parameters for this device are:  $N_D = 3.2 \times 10^{15} \text{ cm}^{-3}$ ,  $q\phi_{BO} = 0.87 \text{ eV}$ ,  $A^{**} = 112 \text{ A cm}^{-2} \text{ } ^\circ\text{K}^{-2}$ ,  $D = 1.8 \times$

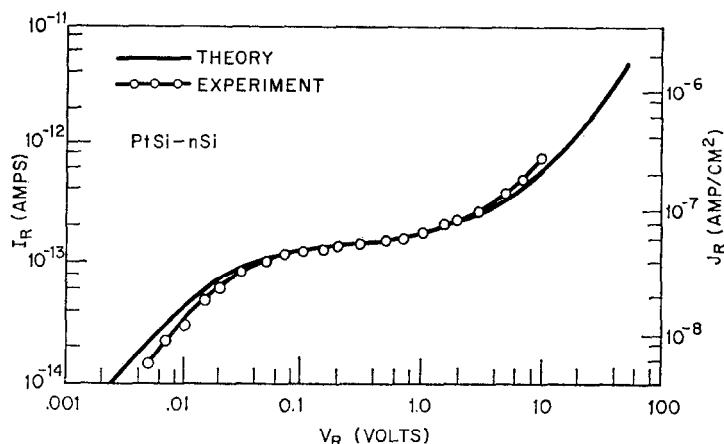


FIG. 10. Reverse characteristics of PtSi Schottky diode formed in *n*-type silicon with long minority carrier lifetime (32  $\mu$ sec). Measurements were carried out at room temperature.

$10^{-3}$  cm,  $\alpha = 30 \text{ \AA}$ ,  $T = 297^\circ\text{K}$ . Reverse characteristics of PtSi formed in *p*-type silicon are nearly ohmic over five orders of magnitude of applied bias. This is caused by a combination of low barrier height (0.25 eV) and large series resistance. These data<sup>(4)</sup> will not be reproduced here.

#### 4. CONCLUSIONS

Experimental measurements of the reverse characteristics of metal-silicide Schottky diodes agree with a unidirectional theoretical model. The typical soft behavior has been interpreted in terms of a fundamental dependence of the effective barrier height on the electric field at the metal-semiconductor interface. The barrier lowering mechanism appears to be characterized by both dynamic (image-force) and static (dipolar charge layer) aspects. The image-force correction is proportional to  $\mathcal{E}_m^{1/2}$ ; the dipolar correction can be approximately represented by a term linear in electric field. The latter, dipolar barrier lowering mechanism is a salient feature of the new model that has been presented, and is thought to be implicit in all metal-semiconductor interfaces whether in intimate contact or separated by a thin, semi-insulating layer of oxide or other contaminant. In the nonideal case of an intervening oxide layer, the analysis [equations (8-10)] suggests that the effect of the additional dipolar barrier lowering

mechanism could be masked by a high density of surface states. This is a plausible interpretation of the experimental results of SZE, *et al.*,<sup>(13)</sup> who measured a barrier height at a Au-*n*Si interface that exhibited a field dependence characterized by image-force alone.

The theoretical model presented also includes a calculation of effective Richardson constants for both *n*- and *p*-type silicon, incorporating anisotropy of the effective mass of the carriers, scattering by optical phonons, and quantum mechanical reflection and tunneling. Although slightly dependent upon electric field, effective Richardson constants for silicon can be approximated by 112 and 32 A/cm<sup>2</sup>/°K<sup>2</sup> for electrons and holes, respectively. These values are correct to an accuracy of  $\pm 6$  per cent for typical electric fields encountered in Schottky barrier devices.

Experimental observations have been made on Schottky diodes composed of three metallic silicide compounds, ZrSi<sub>2</sub>, RhSi and PtSi. Fabricated by solid-solid reaction in both *n*- and *p*-type silicon, these materials form six distinct barrier heights spanning 0.6 eV (see Table 2). The data presented covers five orders of magnitude in reverse bias and eleven orders of magnitude in reverse current density. Quantitative agreement with the theoretical model is obtained for fixed temperatures ranging from 276 to 344°K, with

rms deviations usually less than 10 per cent for all reverse bias values up to the onset of avalanche or tunneling breakdown. Experiments on diodes with different diameters show that reverse currents are proportional to the active area of the device. For the highest barrier device investigated (PtSi-*n*Si), silicon with long minority carrier lifetime ( $32\ \mu\text{sec}$ ) is required in order for the leakage current to be controlled by thermionic emission. Otherwise generation in the depletion region dominates the reverse characteristics.

Further experiments on metallic silicide Schottky diodes should be carried out utilizing photoelectric emission over the barrier to confirm the electric field dependence of the barrier height. The success of a unidimensional theory for Schottky diodes of this improved structure also suggests that better quantitative data on avalanche and tunneling breakdown should be possible.

*Acknowledgements*—The authors would like to express their appreciation to R. M. RYDER for his encouragement and critique of the manuscript. Additional advice contributed by R. J. STRAIN has also been helpful. The authors have benefited from technical discussions with S. M. SZE and C. R. CROWELL. Device fabrication is due to R. W. MACDONALD and P. A. BYRNES. Experimental measurements were carried out by A. LOYA and S. J. KOCSEI.

## REFERENCES

1. J. M. ANDREWS and M. P. LEPSALTER, Paper presented at IEEE International Electron Devices Meeting, Washington, D.C., October 1968.
2. G. H. PARKER, T. C. MCGILL, C. A. MEAD and D. HOFFMAN, *Solid-St. Electron.* **11**, 201 (1968).
3. A. M. COWLEY and S. M. SZE, *J. appl. Phys.* **36**, 3212 (1965); C. R. CROWELL, H. B. SHORE and E. E. LABATE, *J. appl. Phys.* **36**, 3843 (1965).
4. M. P. LEPSALTER and J. M. ANDREWS, *Ohmic Contacts to Semiconductors*, p. 159, B. SCHWARTZ (Ed). Electrochem. Soc. (1969).
5. M. P. LEPSALTER and S. M. SZE, *Bell Syst. tech. J.* **47**, 195 (1968).
6. S. DUSHMAN, *Rev. mod. Phys.* **2**, 381 (1930); F. SEITZ, *The Modern Theory of Solids*, p. 161. McGraw-Hill, New York (1940).
7. C. R. CROWELL, *Solid-St. Electron.* **8**, 395 (1965); **12**, 55 (1969).
8. C. R. CROWELL and S. M. SZE, *Solid-St. Electron.* **9**, 1035 (1966); C. R. CROWELL and S. M. SZE, *Physics of Thin Films*, Vol. 4, p. 325, G. Hass and R. E. Thun (Eds). Academic Press, New York (1967).
9. J. M. ANDREWS (unpublished).
10. C. R. CROWELL and S. M. SZE, *J. appl. Phys.* **37**, 2683 (1966).
11. S. M. SZE, *Physics of Semiconductor Devices*, p. 389. Wiley-Interscience, New York (1969).
12. J. M. ANDREWS, to be published.
13. S. M. SZE, C. R. CROWELL and D. KAHNG, *J. appl. Phys.* **35**, 2534 (1964).
14. C. T. SAH, R. N. NOYCE and W. SHOCKLEY, *Proc. Inst. Radio Engrs* **45**, 1228 (1957).